FREQUENCY RESPONSES OF ALUMINUM A356 BASED ON

HIGH STRENGTH ALLOY COMPOSITE (HSA$_P$)

MAHER REHAIF KHUDHAIR[1] & M. GOPI KRISHNA MALLARAPU[2]

[1]Research Scholar, Department of Machine Design, Acharya Nagarjuna University, Guntur, Andhra Pradesh, India

[1]Al-Furat Al-Awsat Technical University, Iraq

[2]Department of Mechanical Engineering, Acharya Nagarjuna University, Andhra Pradesh, India

ABSTRACT

MMCs are promising materials under constant development and their application in different industries is increasing. Aluminum is one such pioneer materials which is being used extensively in aerospace, automotive and the manufacturing industry. In the present study an analysis tool finite element analysis (FEA) will be used. The work presented in this paper is aimed at the study of vibration characteristics of aluminum A356 with different reinforcements. A356 alloy and Al–20Cu–10Mg alloy system has been investigated as matrix and reinforcements. Modulus of elasticity of composites was found from tensile test, and the samples are synthesized through stir casting technique by dispersing high strength alloy particulates (HSA$_P$) quickly and continuously to the vortex, and ingot into a Cast Iron cylindrical mould. Homogenized billets were hot extruded into ϕ 14 mm rod form. Density of the composites found to be increasing with increases weight ratio of reinforcements which is in tune with the calculated values by rule of mixtures, a variation densities among A356 Alloy and weight ratio (5%–10%–15%) reinforcements has been observed. Modeling of the samples using Solids Works 2013 and a modal analysis carried out using ANSYS software v.14.5, to understand the vibration behavior of the composite materials. Which play an important role in the design of dynamic machines. The harmonic analysis has done to determine the natural frequencies and the mode shapes of composite materials where evaluated and compared. The study showed that the effect of density and modulus of elasticity mainly on the vibration characteristics of the composite material where the natural frequency increases to increase the modulus of elasticity. The decrease of density causes the frequency increases of the samples, as well as the second moment of area has Influence on the vibration characteristics. The results are evident that vibration properties is higher for A356–10% in comparison with (A356 alloy, A356–5%, and A356–15%).

KEYWORDS: MMCs, Aluminum A356, Natural frequency, Mode shape, Displacement

INTRODUCTION

The word composite in the term composite material signifies that two or more materials are combined on a macroscopic scale to form a useful third material. The key is the macroscopic examination of a material wherein the components can be identified by the naked eye. Different materials can be combined on a microscopic scale, such as in alloying of metals, but the resulting material is, for all practical purposes, macroscopically homogeneous, i.e., the components cannot be distinguished by the naked eye and essentially act together [1]. Continuously developing technologies contribute to improvements in materials science. Composite materials have now replaced traditional engineering materials. The production of composite materials and the development of subsequent shaping processes have

become very relevant for technological applications.[2]

Classification and Characteristics of Composite Materials

Composites are commonly classified at two distinct levels. The first level of classification is usually made with respect to the matrix constituent The major composite classes include organic–matrix composites (OMCs), metal–matrix composites (MMCs), and ceramic–matrix composites (CMCs). The term "organic-matrix composite" is generally assumed to include two classes of composites: polymer–matrix composites (PMCs) and carbon-matrix composites.[3] The second level of classification refers to the reinforcement form–particulate reinforcements, whisker reinforcements, continuous fiber laminated composites, and woven composites. In order to provide a useful increase in properties, there generally must be a substantial volume fraction (10% or more) of the reinforcement.

Metal matrix composites (MMCs), as the name implies, have a metal matrix. MMCs exhibit a combination of metallic (toughness and formability) and ceramic (high strength and hardness with load bearing capacity) properties. These are tailor made materials to suit to particular requirements like reduction in density or improvement in stiffness, yield strength, ultimate tensile strength, which can be translated to improved specific properties. Depending on the application, a wide range of composites with different combinations of matrix materials and dispersoids are being produced. Table1 gives a glimpse of the types of matrices and dispersoids used for various applications [4]. Initial investigations were made with process development using fibre reinforcement. Anisotropy, expensive fabrication cost and restricted secondary processing has led to the use of short fibre/particulate/whisker reinforced composites. The combination of good transverse properties, low cost high workability and significant increase in performance over unreinforced alloys are the commercially attractive features of these discontinuous reinforced composites. Compared to dispersion strengthened systems, particulate reinforced composites contain coarse size reinforcement (1–100 μm) in relatively high weight fractions (1–30%). In particulate composites, both matrix and reinforcement.

Table 1: MMCs Components and their Applications [4]

Composite*	Components	Benefits
Al- SiC$_{(p)}$	Piston	Reduced weight, high strength and wear resistance
	Brake rotor, caliper, linear	High wear resistance and reduced weight
	Propeller shaft	Reduction of weight and high specific stiffness
Al- SiC$_{(w)}$	Connecting rod	Reduced reciprocating mass, high specific strength, stiffness and low CTE
Al- SiC$_{(p)}$	Sprockets, pulleys, covers	Reduced weight, high strength and stiffness
Al- Al$_2$O$_{3(sf)}$	Piston ring	Wear resistance and high running temperature
	Piston crown	Reduced reciprocating mass, high creep and fatigue resistance
Al- Al$_2$O$_{3(lf)}$	Connecting rod	Reduced reciprocating mass, improved strength
Cu-graphite	Electrical contact strips, electronic packaging, bearings	Low friction and wear low CTE
Al- graphite	Cylinder, linear, piston bearing	Gall resistance reduced friction, wear and weight
Al- TiC$_{(p)}$	Connecting road, piston	Reduced weight and wear
Al-fiber frax	Piston	Reduced weight and wear
Al- Al$_2$O$_{3(f)}$- C$_{(f)}$	Engine block	Reduced weight, improved strength and wear resistance

Metallic Fibers

Metallic fibers include fibers made from a variety of base metals and alloys. By processing the raw material into fibers of small dimensions of the order a µm, flaws inherent in the bulk material are virtually eliminated and enhanced properties are achieved. The fiber strength is directly related to the fiber diameter, that is in turn related to the fiber manufacturing cost.[5]

A number of metals are available in various fiber form, in theory providing a pool from which desirable properties may be extracted for any application. However in reality, a number of practical factors limit the number of fiber types that are feasible, especially for polymer composite applications, where mechanical properties are particularly important. The most important of these are:[6] bear substantial load. In addition, matrix strength as affected by precipitation and dislocation strengthening plays an important role in the load bearing capacity of these composites. Metal matrix composites reinforced with ceramic particles are widely used due to their high specific modulus, strength and wear resistance, (Table 1).

Bear substantial load. In addition, matrix strength as affected by precipitation and dislocation strengthening plays an important role in the load bearing capacity of these composites. Metal matrix composites reinforced with ceramic particles are widely used due to their high specific modulus, strength and wear resistance, (Table 1).

MATERIALS AND METHODS

Metal matrix composites (MMCs) consist, a pure metal or alloy as matrix material, and the reinforcement as particulates, whiskers or continuous fiber. Metal matrix composites possess some attractive properties which include elevated temperature applications, high transverse strength, high electrical conductivity, and superior thermal conductivity and high wear resistance. Depending upon the application in service, a variety of composites with different combinations of matrix materials and reinforcements are being produced through different fabrication methods [7].

Selection of Matrix Material

A356–Al–Si is a binary alloy with 6.5% Si and small amounts of Cu, and other common elements. This alloy has a great importance in engineering industries, as it exhibit high strength to weight ratio, high wear resistance, low density, low coefficient of thermal expansion etc. Silicon imparts high fluidity and low shrinkage, which result in good castability, weldability. Presence of high hard silicon particles, improve wear resistance. The properties of casting alloy A356 are outlined in table 2. The Al–Si system, figure 1, has a eutectic reaction at 577 ºC and a eutectic composition of 12.6 wt%. As aluminum and silicon solidify in different structures, respectively face centered cubic (FCC) and diamond cubic, two solid phases, α and β are produced. At high temperature, the hypoeutectic alloy forms a rich aluminum α- phase solid. The hypereutectic alloy forms almost pure β phase silicon. Very little silicon (1.65 wt%) dissolves in the α phase aluminum and almost negligible amount of aluminum dissolves in the $β$ phase, figure 2 shows the microstructure of A356 alloy at 200x magnification.[8]

Table 2: Properties of A356 Casting Alloy [8]

Tensile Strength	221–262 MPa
Yield Strength	165–185 MPa
Elastic Modulus	72.4 GPa
Hardness	70–80 HB
Density	2.685Kg/m^3
Liquidus Temperature	615 ºC
Solidus Temperature	577 ºC
Coefficient of Thermal Expansion	23.5μm/m.K at 20–300 ºC
Thermal Conductivity at 25 ºC	151–155W/m.K
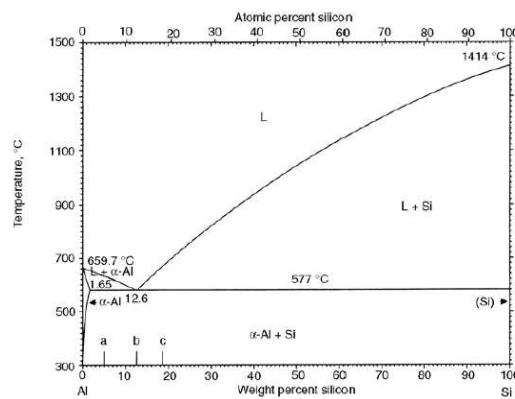
Figure 1: Al–Si Phase Diagram [9]
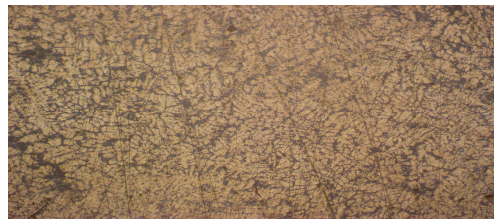
Figure 2: Microstructure of A356 Alloy at 200x Magnification

The alloy used in this study is A356, which is a widely used aluminum casting alloy. It has very good mechanical strength, ductility, hardness, fatigue strength, pressure tightness, fluidity, and machinability. This alloy is used in many industrial applications such as airframe castings, machine parts, truck chassis parts, aircraft and missile components, and structural parts requiring high strength [10]. In the present investigation, A356 alloy (a commercial alloy), supplied by M/s Synergies Dooray automotives limited, Visakhapatnam, was used as matrix material and the chemical composition was shown in table 3.

Table 3: Chemical Composition of A356 Alloy, Wt. %

Si	Mg	Cu	Ti	Zn	Fe	Al
6.5	0.4	0.05	0.06	0.03	0.09	Balance

Selection of Reinforcement Material

Aluminum–Copper–Magnesium alloys are excellent strength vs. density ratio, formability and corrosion resistance, make high–copper Al–Cu–Mg alloys a potential candidate for a number of industrial applications. Developed in

the early times in the aeronautical field, they have been then considered for a wide range of different applications, even though, due to their high specific strength, they are mainly considered as a substitute of iron–based materials for structural parts in the transportation industry. Several technical compositions are presently standardized and new alloys based on that metallic system are now being considered and developed [11]. The prime idea of fabrication for a strong and wear resistant reinforcement, compatible with matrix material needs to be investigated for composite preparation. A series of alloys have been prepared and investigated for suitability as reinforcement.

Characterization of Reinforcement Material
Hardness Studies

Copper plays an important role in strengthening the base matrix. In addition, it substantially increases the wear resistance of the resulting composite [12, 13]. Initial trials with binary alloys of aluminum have shown increase in hardness from 45 to 144 VHN, with increased Cu contents, figure 3 (a). J B Rao [14] reported that Al–Cu binary alloys with increasing copper contents up to 6% show increased hardness values. Similarly Al-Cu-Mg in ternary alloys with increasing Mg contents up to 2%, show increased hardness. In order to achieve higher hardness values, ternary alloy systems have been tried with higher magnesium contents. Al-10Cu with 10Mg and 20Mg has shown further increase in hardness from 96 to 198 VHN figure 3 (b).
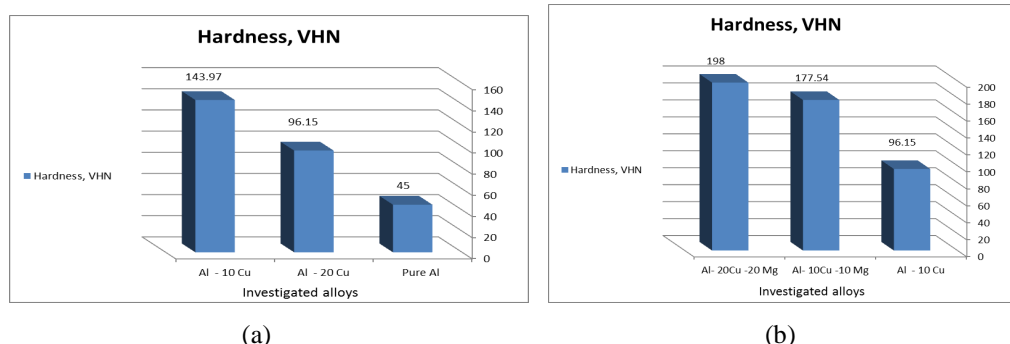

(a)   (b)

Figure 3 (a) Hardness Behaviour of Investigated   (b) Hardness Behaviour of Investigated
Binary Alloys with Increase in Cu Content,   Ternary Alloys

Though higher hardness values (254 VHN) have been achieved with Al–20Cu–20Mg, figure 4, lack of fluidity of the composition, limited its adaptability as reinforcement.
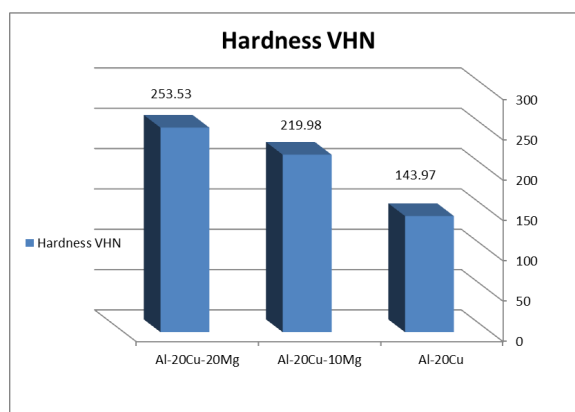

Figure 4: Hardness Behaviour of Investigated Alloys with Increase in Mg Content

Specific Hardness

Specific hardness of the alloys was calculated by dividing hardness with density of the corresponding alloy, for Al–10Cu–10Mg the hardness was 37.11, and 58.45 for Al–20Cu–10Mg alloy. From the measured values of specific hardness, Al–20Cu–10Mg alloy was chosen as reinforcement material.

Density Studies of Reinforcement Material

The average theoretical and measured density values of the investigated alloys shown in figure 5. It can be seen that the densities found to be decreasing with increase in magnesium concentrations.
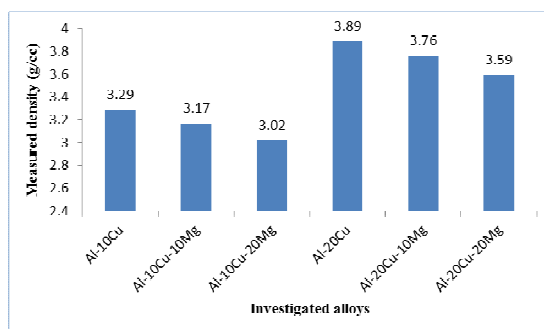
Figure 5: Densities of Investigated Alloys

FABRICATION AND CHARACTERIZATION OF COMPOSITE

Most of the investigations and research in MMCs, prioritized in increasing strength and hardness properties. Presence of hard and brittle reinforcements, restrict the mobility of dislocation, thus enhancing the strength properties. On the other hand, ductility decreases to a great extent, due to lack of interfacial bonding and fracture of reinforcements.

Experimental Work

Fabrication of Composites

All the composites were synthesized through stir casting technique, which is a proven and well established method for composite (MMC) making. A356 alloy was melted in an electric resistance furnace. A temperature of 720^0 C, was maintained throughout the process. The melt (1.5 kg) was thoroughly degassed using Argon, and gas jacket on melt was maintained throughout the process. A vortex was created at an rpm between 700 and 750 using a graphite impeller, preheated (200^OC) high strength alloy particulates ($HSA_{(P)}$) were added quickly (5-15 wt.%) and continuously to the vortex, through a screen. At the end the particulate addition, composite was cast into a cast iron cylindrical mould, figure 6. Hot ingot was transferred to a furnace at 100^OC, and homogenized for 24 hrs.

PROCESS DETAILS

The following are the process parameters for fabrication of composites.

Mould   : Cast Iron, 100 mm length × 60 mm Φ

Degassing with Argon   : One Minute

Furnace temperature   : $720–730^O$C

Inert atmosphere   : Argon gas

Pressure of Argon gas used   : 10–15MPa

Rotational speed of stirrer : 700–750 rpm

Position of stirrer   : 1 inch height from bottom ofcrucible and centrally located

Average particle size   : 125 μm

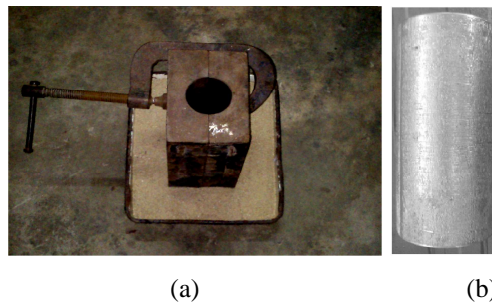Particle preheating temp.   : 200°C.

(a)   (b)
Figure 6: a - Die Used for Composite Preparation b- Cast Ingot

Extrusion of Composites

Surfaces of cast billets were machined, to remove the oxide layer to minimize the friction between the extrusion container and the material. Composite cast billets (wrapped in aluminum foil) were then hot extruded into Φ 14 mm rod (extrusion ratio of 18:1) by maintaining extrusion container at 450 ^{o}C and preheating the billet at 450 ^{o}C for 30mins. All the composites along with the matrix alloy thoroughly homogenized at 100 ^{o}C for 24 hours in an industrial oven, after extrusion process, extruded rods were shown in figure 7.

PROCESS DETAILS

Billet dimensions   : 60 mm height $\times$ 60 mm Φ

Soaking   : 450 ^{o}C, 2 hours

Lubricant   : Molybdenum–Di–Sulphide

Pressure pad temp. : 450 ^{o}C, 20 minutes

Extrusion ratio   : 18:1

Orifice diameter   : 14 mm

Die temperature   : 500 ^{o}C


Figure 7: Extrusion Rods

Density Studies

Density of the composites found to be increasing with weight fractions of the reinforcements added, figure 8, which is intune with the calculated values by rule of mixtures as shown in table 4.

Table 4: Densities of Composites

Material	Theoretical Density (g/cc)	Measured Density (g/cc)	Difference (g/cc)
A 356 alloy	2.680	2.680	0
A356–5 % composite	2.739	2.691	±0.048
A 356–10% composite	2.797	2.728	±0.069
A 356–15% composite	2.856	2.749	±0.107

The difference is found to be increasing with increasing concentrations of reinforcement. This could be attributed to the loss of magnesium, as more stirring times were involved with higher reinforcement content additions.
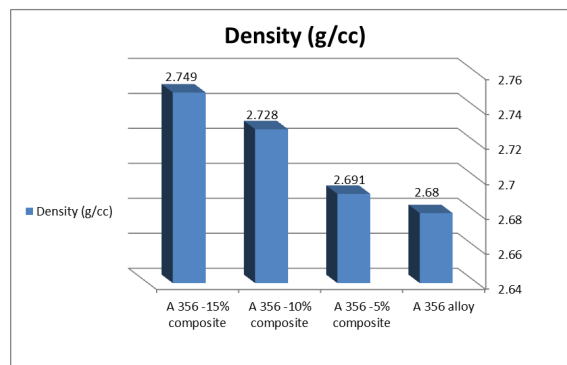
Figure 8: Density of HSA(P) Composites

Hardness Studies

Hardness values of the composites were found to be increasing with increasing reinforcement contents. This can be attributed primarily to the refined grain structure of matrix, presence of harder reinforcement and harder $CuMgAl_2$ phase in the matrix. Also the increase may be due to increase in interfacial area between the matrix and the reinforcement leading to increase in strength appreciably. Composites exhibit improved hardness values compared to the matrix of the alloy, figure 9, hardness found to be increasing with increasing reinforcement content from 54.5 to 91 VHN i.e. 66 %.
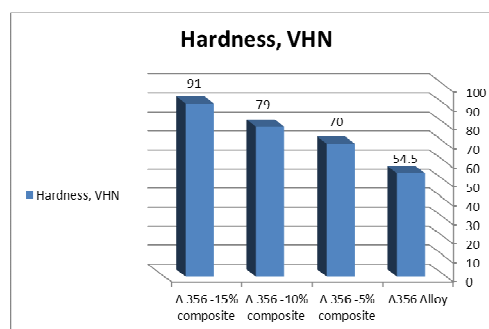
Figure 9: Hardness Variations of Composites

Similar behaviour of increase in hardness with increasing silicon carbide between 5 and 15 wt %, as reinforcement in A356 alloy [15]. Presence of SiC particles which are very hard dispersions contribute positively to the hardness of the composite. The increased hardness is also attributable to the hard SiC particles acting as barriers to the movement of dislocations within the matrix. Howell *et al.* [16] and Vencl et *al.* [17] reasoned the improvement of the hardness of the composites to the increased particle volume fraction. Wu [18] and Deuis [19] attributed this increase in

hardness to the decreased particle size and increased specific surface of the reinforcement for a given volume fraction. Sug Won Kim *et al.* [20] reasoned the increase in hardness of the composites to the increased strain energy at the periphery of particles dispersed in the matrix. Deuis *et al.* concluded that the increase in the hardness of the composites containing hard ceramic particles not only depends on the size of reinforcement but also on the structure of the composite and good interface bonding. If the interfaces are weak, the reinforcement particles can easily be pulled out by the action of the abrasive, leading to considerable material loss.

Tensile Behaviour of Composites

Figure 10 shows the deformation behavior of alloy and the composites under tension. Compared to the alloy, the composites show higher strength values and the strength increases with increasing reinforcement contents.
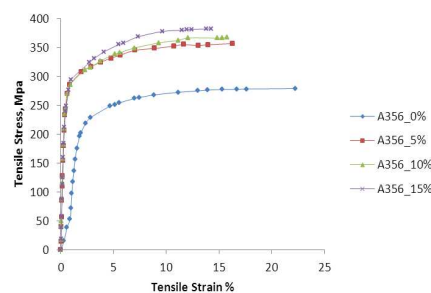

Figure 10: Tensile Stress Vs. Tensile Strain of HAS (P) Composites

Table 5, compares the tensile properties of the alloy and the composites with reinforcements between 5 and 15 %.

Table 5: Comparison of Tensile Behaviour of the Alloy and HAS (P) Composites

% Reinforcement	Young's Modulus of Elasticity, GPa	Ultimate Tensile Strength (UTS), MPa	Yield Strength, MPa	% Elongation
Base A356 (0%)	79.23	279.3	181.21	25.14
5	86.14	357.28	261.53	15.83
10	92.7	367.87	272.22	15.05
15	98.26	383.11	278.85	10.55

The modulus of elasticity increased by 9 to 25% with the addition of 5 to 15% reinforcements. Presence of reinforcement restrict the mobility of the dislocation enhance the modulus to higher values. Similar behaviour was identified by many researchers.

ANALYTICAL SOLUTION FOR TRANSVERSE VIBRATIONS OF BEAM

Model analysis can be classified into three types: analytical, numerical, and experimental solutions. Mathematical models have been developed for analytical and numerical solutions. Analytical solutions can be divided into two types: exact and approximate. Exact solutions can be found for many problems using simplifying assumptions. Approximate solutions typically use fewer assumptions. The difference between exact analytical solutions and approximate analytical solutions is that exact solutions are finite and do not neglect higher order terms. Approximate analytical solutions are typically series, so they are infinite. However, by neglecting higher order terms, a finite solution that is very close to the true solution can be calculated. Numerical solutions can be found for more complex problems, however they can be

plagued by problems of convergence.

Transverse beam vibration, in which the beam vibrates in a direction perpendicular to its length, are also called flexural vibrations or bending vibrations.[21]

We make the following assumptions:

- The beam has uniform properties.

- The beam is slender (h/l and w/l are small).

- The beam material is linear, homogeneous, and isotropic; additionally, it obeys Hooke's law.

- There is no axial load.

- Plane sections remain plane during motion.

- The plane of motion is the same as the beam symmetry plane (so rotation and translation are independent).

- The mass moment of inertia about the z axis is negligible.

- Shear deformation is negligible.

In the initial analysis of bending vibration, we assume that there is no axial force at the ends of the beam. We make further simplifying assumptions, which will be clear in the development of the governing equation of motion. The study of bending vibration (or lateral or transverse vibration) of beams is very important in a variety of practical situations. Noteworthy, here, are the vibration analyses of structures like bridges, vehicle guideways, tall buildings, and space stations; ride quality and structural integrity analyses of buses, trains, ships, aircraft and spacecraft; dynamics and control of rockets, missiles, machine tools, and robots; and vibration testing, evaluation, and qualification of products with continuous members[22]. To begin this discussion, let's consider the bending of beams using Euler–Bernoulli beam theory and see how we can expand the analysis to derive the vibration response. The fundamental relationship between the transverse deflection, y, and a load per unit length, q, applied to a beam1 with constant cross section and material properties is provided in Equation 1. In this equation E is the elastic modulus, I is the second moment of area, and x is the (continuous) position along the beam. Figure 11 displays the x and y coordinate axes for a rectangular beam.[22]

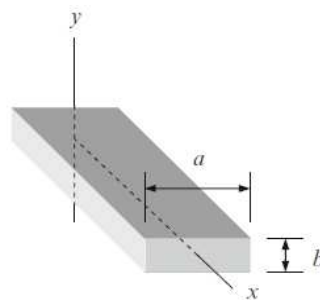$$\frac{q}{EI} = \frac{d^4 y}{dx^4}$$

(Equ. 1)

Figure 11: Coordinate Definitions for Continuous
Beam Transverse Deflection

To determine the static (non–vibratory) deflection of a continuous beam under a selected loading condition, we integrate Equation 1 four successive times. Let's apply the loading condition shown in Figure 5.10, where a simply supported beam with length, *l*, is loaded by a force per unit length, *w*. Due to symmetry, the reaction force, *wl*=2, is the same at both ends. Equation 1 can be rewritten as shown in Equation 2 for this case.

$$\frac{q}{EI} = \frac{d^4 y}{dx^4} = \frac{-w}{EI}$$

(Equ. 2)

Integrating Equation 2 gives Equation 3, where C_1 is the integration constant and *V* is the position–dependent shear force acting on the beam.

$$\frac{V}{EI} = \frac{d^3 y}{dx^3} = \frac{-w}{EI} + C_1$$

(Equ. 3)

Integrating a second time yields the moment, M, equation shown in Equation 4. Now there are two integration constants.

$$\frac{M}{EI} = \frac{d^2 y}{dx^2} = \frac{-w^2}{EI} x + C_1 x + C_2$$

(Equ. 4)

For the beam vibration, we need to determine the time–dependent deflection. We will now build on the previous analysis to determine the required differential equation of motion for the beam. Let us begin with Figure 12, which shows the forces and moments acting on a section of a vibrating Euler–Bernoulli beam with an infinitesimal length, ∂x.

According to Newton's second law, the sum of the forces in the *y* direction is equal to the product of the section mass and acceleration, $\sum F_y = m \frac{\partial^2 y}{\partial t^2}$. See Equation 5, where the mass is rewritten as the product of the density, *ρ*, cross–sectional area, *A*, and section length, ∂x.

$$q\partial x + V(x) - V(x + \partial x) = \rho A \partial x \frac{\partial^2 y}{\partial t^2}$$

(Equ. 5)

We can rewrite Equation 5. The result is provided in Eq. 6.

$$q - \frac{\partial V}{\partial x} = \rho A \frac{\partial^2 y}{\partial t^2}$$

(Equ. 6)
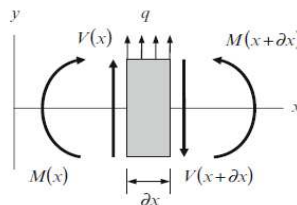
Figure 12: Forces and Moments Acting on a Small Section
of a Vibrating Euler–Bernoulli Beam

From Equation 3, the shear force is $V = EI \frac{d^3 y}{dx^3}$. Calculating the partial derivative with respect to x gives:

$$\frac{\partial V}{\partial x} = EI \frac{\partial^4 y}{\partial t^4}$$

(Equ. 7)

Substituting Equation 7 into 6 gives the differential equation of motion for the transverse vibration of a uniform cross section Euler–Bernoulli beam.

$$\rho A \frac{\partial^2 y}{\partial t^2} + EI \frac{\partial^4 y}{\partial t^4} = q$$

(Equ. 8)

For free vibration, the external transverse load, q, is zero, so we can write:

$$\rho A \frac{\partial^2 y}{\partial t^2} + EI \frac{\partial^4 y}{\partial t^4} = 0$$

(Equ. 9)

4.1 Frequency Response Function for Transverse Vibration

Our next task is to determine the beam's frequency response function using Equation 9. A general solution to this equation is:

$$y(x,t) = Y(x)\sin(\omega t)$$

(Equ. 10)

Where $Y(x)$ is a function that describes the position–dependent vibration behavior and ω is frequency. Now calculate the required partial derivatives of Equation 10 that appear in Equation 9.

$$\frac{\partial^2 y}{\partial t^2} = Y(x).\left(-\omega^2\right)\sin(\omega t)$$

(Equ. 11)

$$\frac{\partial^4 y}{\partial t^4} = \frac{Y^4(x)}{\partial x^4}\sin(\omega t)$$

(Equ. 12)

Substituting Equations 11 and 12 into Equation 9 gives:

$$\left(\rho A\left(-\omega^2 Y\right) + EI \frac{\partial^4 Y}{\partial x^4}\right)\sin(\omega t) = 0$$

(Equ. 13)

Rewriting Equation 13 yields:

$$\frac{\partial^4 Y}{\partial x^4} - \omega^2 \frac{\rho A}{EI} Y = 0$$

(Equ. 14)

Where

$$\lambda^4 = \omega^2 \frac{\rho A}{EI}$$

(Equ. 15)

We now have:

$$\frac{\partial^4 Y}{\partial x^4} - \lambda^4 Y = 0$$

(Equ. 16)

The time–dependence of Equation 9 has been eliminated in Equation 16. In addition, frequency has been introduced through the λ^4 term. A general solution to this new equation is:

$$Y(x) = A.\cos(\lambda x) + B.\sin(\lambda x) + C.\cosh(\lambda x) + D.\sinh(\lambda x) \qquad \text{(Equ. 17)}$$

Cantilever Beam Analysis

Figure 13 shows a fixed–free beam. In order to determine the FRF at the free end, coordinate 1, we need to apply a force, $F_1 = F.\sin(\omega t)$, at this location. Note that the force and vibration, $y(x,t) = Y(x)\sin(\omega t)$, expressions both have the same sinusoidal form. The cantilever base coordinate is labeled as 2. We need to identify four boundary conditions for this beam in order to determine the coefficients *A* though *D* in Equation 17.

For the free end, where *x=l*, no moment is supported (it is free to rotate), so we can modify Equation 17 to be:

$$\left.\frac{M}{EI}\right|_{x=l} = \left.\frac{d^2 y}{dx^2}\right|_{x=l} = 0 \qquad \text{(Equ. 18)}$$
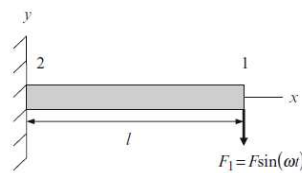
Figure 13: Fixed–Free Beam Model with a Harmonic Force
Applied at the Free End

We know that the shear force at the free end is $F_1 = F.\sin(\omega t)$, so we can define the corresponding boundary condition (see Equation 3).

$$\left.\frac{V}{EI}\right|_{x=l} = \left.\frac{d^3 y}{dx^3}\right|_{x=l} = -\frac{F}{EI}\sin(\omega t) \qquad \text{(Equ. 19)}$$

At the fixed end, *x* = 0, both the deflection and the slope are zero.

$$\left.\frac{d^2 y}{dx^2}\right|_{x=l} = 0 \qquad \text{(Equ. 20)}$$

$$y|_{x=0} = 0 \qquad \text{(Equ. 21)}$$

Now use Equations. 17 through 20 to determine the coefficients in Equation 16

At *x* = 0, we obtain:

The natural frequencies of the beam are computed from equation 15

$$\omega = \lambda^2 \sqrt{\frac{EI}{\rho A}} = (\lambda l)^2 \sqrt{\frac{EI}{\rho A l^4}} \qquad \text{(Equ. 22)}$$

The function *Y(x)* is known as the normal mode or characteristic function of the beam and *ω* is called the natural frequency of vibration. For any beam, there will be an infinite number of normal modes with one natural frequency associated with each normal mode. The value of *λ* in equation 22 can be determined from the boundary conditions of the beam as indicated below:

Free End

$$Bending\ moment = EI\ \frac{\partial^2 w}{\partial x^2} = 0, \quad Shear\ force = \frac{\partial}{\partial x}\left(EI\ \frac{\partial^2 w}{\partial x^2}\right) = 0$$

(Equ. 23)

For Euler–Bernoulli beams, a closed–form expression for the natural frequencies has been developed for various boundary conditions. See Equation 23, where i =1, 2,3… indicates the natural frequency numbers in ascending order.

$$f_{n,i} = \frac{\beta^2}{2\pi l^2}\sqrt{\frac{EI}{\rho A}} \quad (Hz)$$

(Equ. 24)

Where $\beta = \lambda l$, the β_i values are provided in table 6, the natural frequencies did not change! While the wider beam is indeed stiffer, it is also heavier. These effects serve to offset each other so that the natural frequencies are not affected.

Table 6: Boundary Conditions for the Transverse Vibration of a Fixed–Free Beam.[24]

Frequency Equation	Mode Shape (Normal Function)	Value of λl
$\cos(\lambda_n l).\cosh(\lambda_n l) = -1$	$Y_n = C_n[\sin(\lambda_n x) - \sinh(\lambda_n x) - \alpha_n(\cos(\lambda_n x))]$ where $\alpha_n = \frac{\sin(\lambda_n l) - \sinh(\lambda_n l)}{\cos(\lambda_n l) - \cosh(\lambda_n l)}$	$\lambda_1 l = 1.875104$ $\lambda_2 l = 4.6964091$ $\lambda_3 l = 7.854757$ $\lambda_4 l = 10.995541$

EXPERIMENTAL RESULTS

The dimensions and the material constant for a uniform fixed free beam (cantilever beam) studied in this research are: Material of beam = Aluminum A356 with different composition (5%, 10%, and 15% composites), Poisson's ratio 0.33.

Total length l = 800 mm, width b = 20 mm, height h = 5 mm,

Moment of inertia I = 2.08333 × 10^{-10} m^4,

Young's Modulus E = (see table 5).

Density = (Measured Density, see table 4).

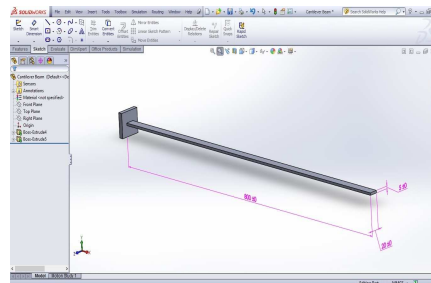Modeling of cantilever beam shown in the figure 14 by using Solid Works program 2013.

Figure 14: Modeling of Cantilever Beam

Putting all required data in Equation 5.96 and we get the four frequencies for four modes as shown in table 6. We shall now investigate the free vibration of fixed free beam using the ANSYS 14.5 program, a comprehensive finite element package.

We use the ANSYS 14.5 structural package to analysis the vibration of fixed free beam. Finite element procedures at present very widely used in engineering analysis. The procedures are employed extensively in the analysis of solid and structures and of heat transfer and fluids and indeed, finite element methods are useful in virtually every field of engineering analysis. The numerical results were found out by using the ANSYS program as shown in Table 7.

Table 7: Natural Frequency (Hz) Using Ansys Program

Reinforcement Sample %	Mode 1	Mode 2	Mode 3	Mode 4
Base A356 (0%)	6.9134	27.641	54.046	215.24
5	7.19383	28.762	56.238	223.97
10	7.4119	29.4119	57.943	230.76
15	7.6018	30.393	59.427	236.67

The figures (15 to 16) describes the natural frequencies and mode shape of the aluminum A356 alloy with different percentage ratio of reinforcement (0% – 5% – 10% – 15%), which appeared in the program ANSYS 14.5.

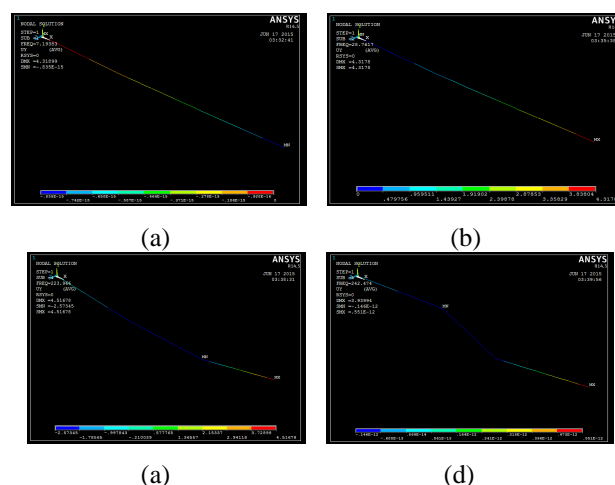(a)　　　　　　　　(b)

(c)　　　　　　　　(d)
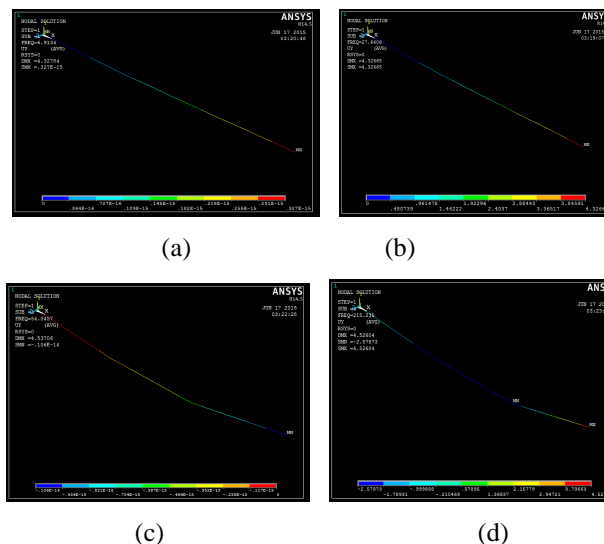
Figure 15: Four Mode Shapes of A356 Alloy

(a)　　　　　　　　(b)

(a)　　　　　　　　(d)

Figure 16: Four Mode Shapes of A356–5% Reinforcement

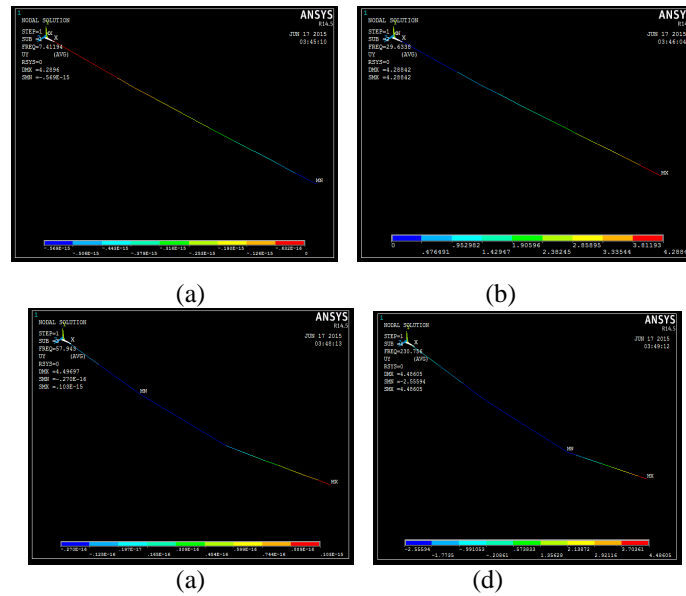(a)   (b)

(a)   (d)

Figure 17: Four Mode Shapes of a356–10% Reinforcement

(a)   (b)

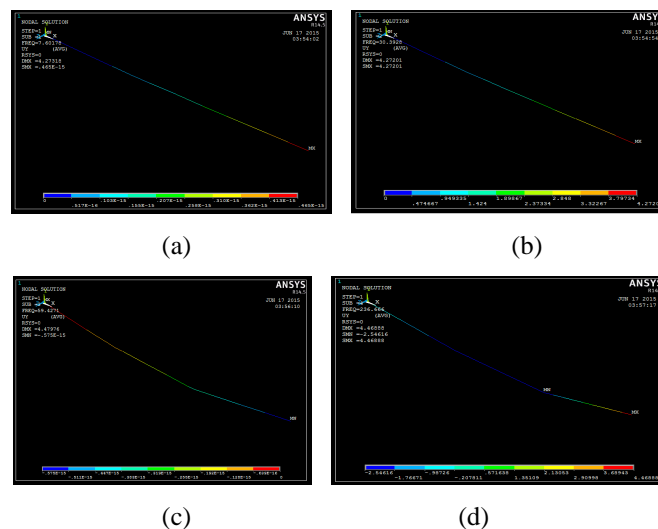(c)   (d)

Figure 18: Four Mode Shapes of A356 – 15 % Reinforcement

Frequency Response Function (FRF)

A harmonic analysis yields solutions of time-dependent equations of motion associated with linear structures under apply harmonic force (100 N cyclic load is applied at the free end), all displacements are to vary with different frequencies. The following graphs were obtained from harmonic analysis as shown in figures (19 to 22).

The Figures (19–22) shows the FRF (Frequency Response Function) plots between displacement and frequency of different specimens. These graphs are plotted by harmonic analysis done in ANSYS. From these graphs natural frequency was calculated. This is basically theoretical modal analysis done in ANSYS.
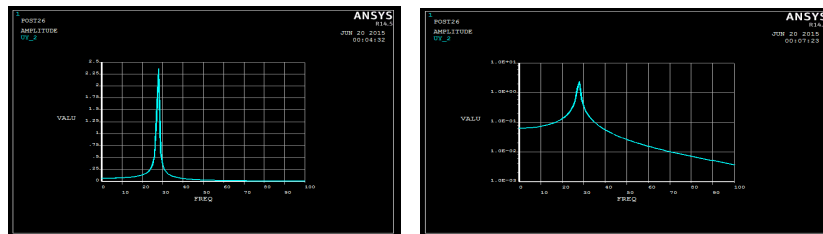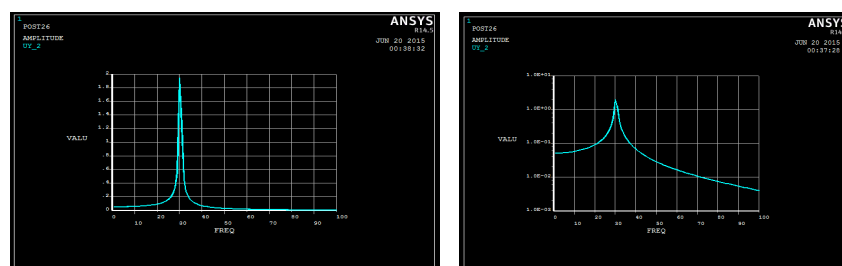
a- Linear Scale with Respect y–Axis   **b- logarithmic Scale with Respect y–Axis**

Figure 19: FRF Graph of A356 Alloy
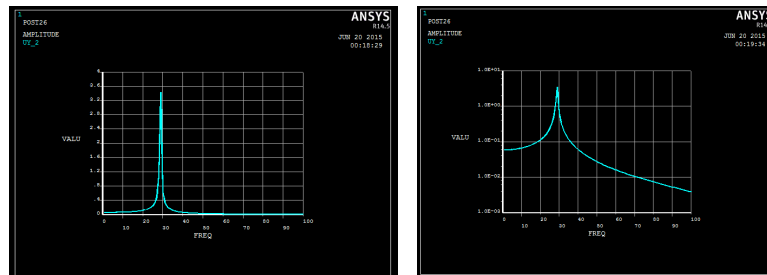
a- Linear Scale with Respect y–Axis   **b- Logarithmic Scale with Respect y–Axis**

Figure 20: FRF Graph of A356 Alloy with 5 % Reinforcement
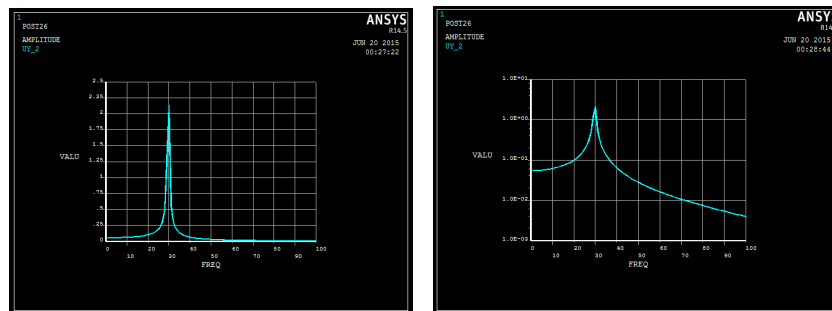
a- Linear Scale with Respect y–Axis   **b- Logarithmic Scale with Respect y–Axis**

Figure 21: FRF Graph of A356 Alloy with 10 % Reinforcement

a- Linear Scale with Respect y–Axis   **b- Logarithmic Scale with Respect y–Axis**

Figure 22: FRF Graph of A356 Alloy with 15 % Reinforcement

RESULTS AND DISCUSSIONS

The numerical results were found out by using the ANSYS program as shown in Table 7. The numerical study using the ANSYS program allows investigates the free vibration of cantilever beam to find out mode shape and their frequencies with high accuracy. The natural frequencies of different specimens (A356 with different reinforcement ratio) which were calculated numerically are compared with each other and results are discussed and shown with the help of bar charts as following:
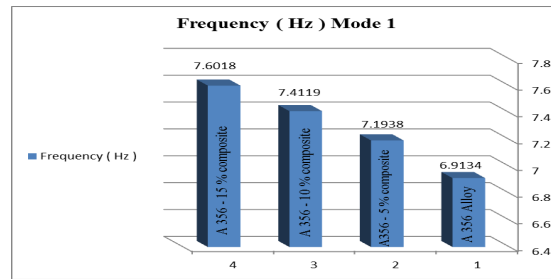
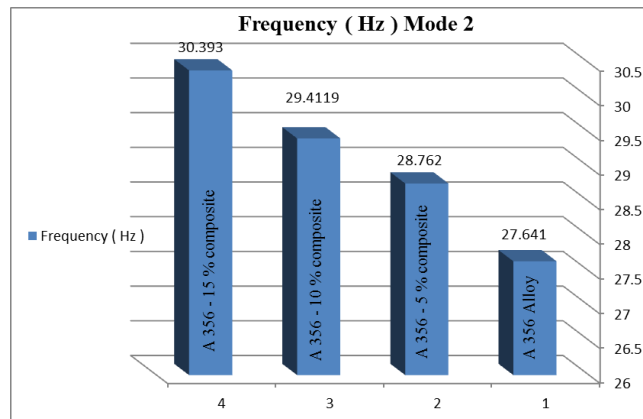**Figure 23: Frequency (Hz) Mode 1**

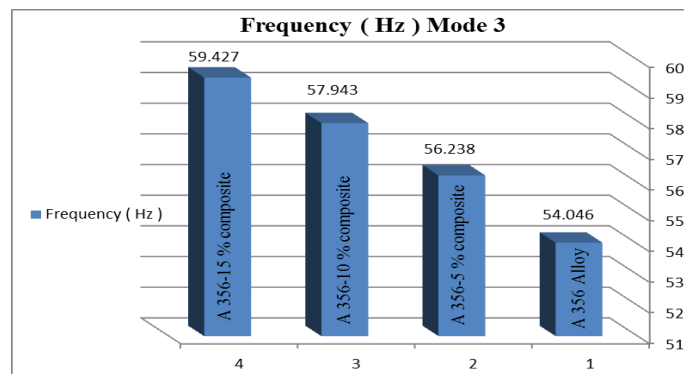**Figure 24: Frequency (Hz) Mode 2**

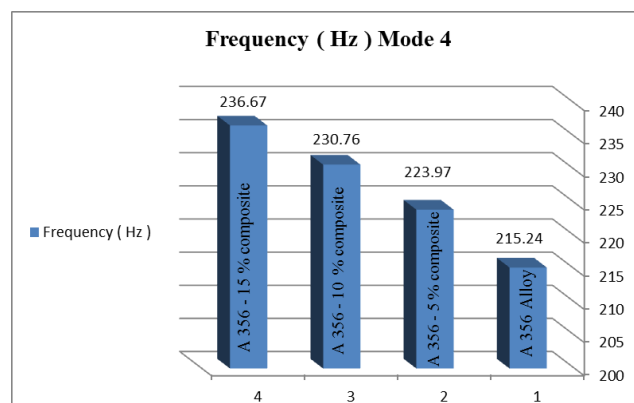**Figure 25: Frequency (Hz) Mode** 3

Figure 26: Frequency (Hz) Mode 4

As seen from the numerical investigation, the natural frequency increases as the increase in density and Modulus of Elasticity for the same dimension of beams for different materials. But decrease in length increases the natural frequency of the beams. Frequency response function under the harmonic force (Figures 19 to 22) can be observed displacement values about y-axis as shown the table 8.

Table 8: Y– Component Displacement of Cantilever Beam

Reinforcement Sample %	Frequency Hz	Minimum displacement	Maximum displacement
Base A356 (0%)	1 – 100	− 1.35593	2.36985
5	1 – 100	− 1.09328	3.43028
10	1 – 100	− 1.25455	2.1321
15	1 – 100	− 1.94972	1.23913

CONCLUSIONS

This research work presents a simple procedure to obtain the natural frequency and mode shape of Euler's Bernoulli beam of rectangular cross section. We obtained the equation for mode shape frequency theoretically and the numerical study using the ANSYS program v. 14.5 allows investigates the free vibration of fixed free beam to find out mode shape and their frequencies with high accuracy.

On the basis of present study following conclusions are drawn:

- The increase in natural frequency could be correlated to the stiffness of materials.

- The natural frequency decreases with increases in density for each material.

- The natural frequency increases with increases in second moment of area.

- The displacement (from end point–node 2) increases with increases in percentage ratio of reinforcements.

- From the experiment it is evident that vibration properties is higher for A356–10% in comparison with (A356 alloy, A356–5%, and A356–15%).

ACKNOWLEDGMENTS

REFERENCES

1. Robert M. Jones, Mechanics of composite Materials, Second Edition, 1999, p.(2).

2. Ibrahim Sahin and Aysegul Akdogan Eker, Analysis of Microstructures and Mechanical Properties of Particle Reinforced AlSi₇Mg₂ Matrix Composite Materials, Journal of Materials Engineering and Performance, Volume 20, No. 6, August 2011, pp. (1090–1096).

3. Daniel B. Miracle and Steven L. Donaldson, Miracle and S.L. Donaldson, Air force research laboratory, pp. (1–2).

4. S. Ray, Review: Synthesis of cast metal matrix particulate composites, Journal of Materials Science, Vol.28, 1993, pp. (5397–5413).

5. Ever J. Barbero, Introduction to composite materials design, second Edition 2011, p.(37).

6. Tahira Jabeen Ahmed, Hybrid Composite Structures: Multifunctionality Through Metal Fibers An exploratory investigation, PHD thesis, 2009, p. (7).

7. M. Gopi Krishna, K. K. Kishore, K. Praveen Kumar, J. Babu Rao, and N.R.M.R. Bhargava, Studies on Deformation Behaviour of A356/Al–20Cu–10Mg Particulate Composite Metallic Materials, International Journal of Engineering Research and Technology (IJERT), ISSN: 2278–0181, Vol. 1 Issue 10, December 2012, pp. (1–6).

8. Gopi Krishna Mallarapu, Metal–Metal Composites: An Innovative Way For Multiple Strengthening, PHD thesis 2013, pp. (1,21,36).

9. Malgorzata Warmuzek, Aluminum–Silicon Casting Alloys: Atlas of Microfractographs (#06993G), ASM International 2004, p.(2).

10. Hao Yu, Processing Routes for Aluminum based Nano–Composites, Master thesis 2010, p. (7).

11. Biljana Zlaticanin, Branislav Radonjic, and Mirjana Filipovic, Characterization of Structure and Properties of As–cast Al–Cu–Mg Alloys, Journal of Materials Transactions, Vol. 45, No. 2, 2004, pp. (440–446).

12. Krishna K. Chawla, Composite Materials Science and Engineering, Second Edition, Springer (India) 1998, pp. (164–165).

13. John E. Hatch, Aluminum Properties and Physical Metallurgy, Vol. 110, 2005, p.(47).

14. J. Babu Rao, Studies on Flow Behaviour of Aluminum, Aluminum–Copper and Aluminum–Copper–Magnesium Alloys During Cold Upsetting Using Vision System, PHD thesis, 2006.

15. Mohan Vanarotti, SA Kori, BR Srdhar, and Shrishail B. Padasalgi, Synthesis and characterization of aluminum alloy A356 and silicon carbide metal matrix composite, International Conference on Industrial Technology and Management, DOL:10.7763/PCSIT. 2012, Vol. 49.3.

16. G. J. Howell, and A. Ball, Dry sliding wear of particulate–reinforced aluminum alloys Against Automobile Friction Materials, Wear Vol. 181–183, February 1995, pp. (379–390).

17. Vencl, I. Bobic, and Z. Miskovic, Effect of thixocasting and heat treatment on the tribological properties of hypoeutectic Al–Si alloy, Wear Vol. 264, Issues 7–8, 15 March 2088, pp. (616–623).

18. J. M. Wu, and Z. Z. Li, Contributions of the particulate reinforcement to dry sliding wear resistance of rapidly of solidified Al–Ti alloys, Wear Vol. 244, Issues 1–2, August 2000, pp. (147–153).

19. R. L. Deuis, C. Subramanian, and J. M. Yellup, Abrasive wear of aluminum composite–A review, Wear Vol. 201, Issues 1–2, 15 December 1996, pp. (132–144).

20. Sug Won Kim, Ui Jong Lee, Sang Won Han, Dong Keun Kim, and K. Ogi, Heat treatment and wear characteristics of Al/SiC_p composites fabricated by duplex process, Composites Part B: Engineering, Volume 34, Issue 8, 1 December 2003, pp. (737–745).

21. William J. Palm, Mechanical Vibration, Wiley India (P.)Ltd., 2010, pp.(619–620).

22. Sondipon Adhikari, Damping Models for Structural Vibration, PDH thesis, 2000, p. (1).

23. Tony L. Schmitz, K. Scott Smith, Mechanical Vibrations: Modeling and Measurement, Springer, 2012, pp. (280–294).

24. Singiresu S. Rao, Mechanical Vibrations, Fourth Edition, 2004, pp. (642–643).